OPEN

Immunology and Cell Biology (2015) 93, 461–471

www.nature.com/icb

ORIGINAL ARTICLE

STAT3 signaling contributes to the high effector activities of interleukin-15-derived dendritic cells

Starlyn Okada[1,3], Shuhong Han[1,3], Ekta S Patel[1], Li-Jun Yang[2] and Lung-Ji Chang[1]

Dendritic cells (DCs) are important innate and adaptive immune effectors, and have a key role in antigen presentation and T-cell activation. Different lineages of DCs can be developed from hematopoietic progenitors following cytokine signaling, and the various lineages of DCs display distinct morphology, phenotype and functions. There has been limited information on differential cytokine-mediated molecular signaling in DCs. Analyses of surface molecules by flow cytometry and quantitative RNA profiling revealed differences between DCs derived from interleukin-4 (IL-4) versus IL-15 signaling, yet both lineages of DCs exhibited similar levels of surface molecules key to immune activation. Functional assays confirmed that IL-15-derived DCs elicited greater antigen-specific, primary and secondary CD8 and CD4 T-cell responses than did IL-4-derived DCs. Importantly, IL-15 DCs secreted substantial amounts of proinflammatory cytokines, including IL-6, interferon-γ (IFN-γ) and tumor necrosis factor-α (TNFα), which helped polarize a strong T-cell response. Assessment of signaling pathways revealed that IL-15 DCs exhibited a lower levels of activated signal transducer and activator of transcription 5 (STAT5), STAT6 and extracellular signal-regulated kinase 1/2 than IL-4 DCs, but after lipopolysaccharide (LPS)/TNFα treatment, the STAT3 and p38 mitogen-activated protein kinase (MAPK) activities were significantly enhanced in the IL-15 DCs. Surprisingly, contrary to the canonical IL-15-mediated STAT5 signaling pathway in lymphoid cells, IL-15 did not mediate a strong STAT5 or STAT3 activation in DCs. Further analysis using specific inhibitors to STAT3 and p38 MAPK pathways revealed that the STAT3 signaling, but not p38 MAPK signaling, contributed to IFN-γ production in DCs. Therefore, while IL-15 does not promote the STAT signaling in DCs, the increased STAT3 activity after LPS/TNFα treatment of the IL-15 DCs has a key role in their high IFN-γ effector activities.
Immunology and Cell Biology (2015) **93,** 461–471; doi:10.1038/icb.2014.103; published online 13 January 2015

Dendritic cells (DCs) are antigen (Ag)-presenting cells essential for initiating and regulating innate and adaptive immune responses. Under normal conditions, immature DCs (imDCs) reside in peripheral tissues. Upon Ag uptake and exposure to proinflammatory cytokines, they undergo maturation and migrate to local lymph nodes. This process is accompanied by morphological and functional changes including upregulation of class I and class II major histocompatibility complex (MHC) and costimulatory molecules, as well as secretion of inflammatory cytokines and chemokines.[1–3] In recent years, attention has been focused on the possibility that tissue microenvironment could markedly influence the phenotype and function of DCs. Further understanding of the differential effects of cytokines on DC development and characterization of molecular mechanisms underlying DC's immune effector functions are crucial to DC immunobiology.

Various environmental stimuli can drive DC progenitors to differentiate into functionally different DC subsets.[2,4–6] The most common method used in generating DCs *in vitro* is differentiating peripheral blood monocytes using IL-4 and granulocyte–macrophage colony-stimulating factor (GM-CSF) (IL-4 DCs). To modify the immune-stimulatory functions of DCs, other cytokines have also been evaluated for DC induction. So far, only IL-15, alone or in combination with GM-CSF, has been reported to induce differentiation of peripheral blood monocytes or cord blood $CD34^+$ precursor cells into functional DCs.[7–12] IL-15 is produced by a range of cell types in response to inflammatory stimuli *in vivo* and has been shown to be important in the maintenance of memory $CD8^+$ T cells and activation of natural killer (NK) cells.[12–14]

Previous studies of IL-15 DCs have focused on $CD8^+$ T-cell immune responses against tumor Ags.[9,10] We have reported that IL-15 can efficiently induce DC differentiation from hematopoietic progenitor/stem cells.[15] However, there is limited information as to how IL-15 drives DC immune effector maturation. IL-15 DCs activate a strong memory T-cell response, but its role in activating naive T cells and NK cells is not well characterized. Furthermore, the molecular events regulated by GM-CSF and IL-15 that drive DC differentiation and polarize their immunostimulatory functions are unknown. In this study, we have performed a comprehensive analysis using donor-matched IL-4 and IL-15 DCs for Ag presentation, costimulation,

[1]Department of Molecular Genetics and Microbiology, College of Medicine, University of Florida, Gainesville, FL, USA and [2]Department of Pathology and Laboratory Medicine, College of Medicine, University of Florida, Gainesville, FL, USA
[3]These authors contributed equally to this work.
Correspondence: Professor L-J Chang, Department of Molecular Genetics and Microbiology, College of Medicine, University of Florida, 1200 Newell Drive, ARB R1-252, Gainesville, FL 32610, USA.
E-mail: lchang@mgm.ufl.edu
Received 28 March 2014; revised 4 November 2014; accepted 13 November 2014; published online 13 January 2015

effector cytokine and chemokine responses, as well as their ability to stimulate autologous CD4 T cells, CD8 T cells and NK cells. In addition, we have characterized the activities of IL-15 DCs in the initiation and maintenance of immune effector responses. Analysis of molecular signaling pathways by intracellular phosphoflow cytometry revealed that IL-15 does not invoke signal transducer and activator of transcription 5 (STAT5) signaling; instead, it increases p38 mitogen-activated protein kinase (MAPK) and STAT3 activities that underlie the strong immune effector functions of IL-15 DCs.

RESULTS

IL-15 drives DC differentiation with a predominant adherent phenotype

The appearance of DCs generated with IL-15 showed obvious differences from the more conventionally IL-4-induced DCs, which was apparent in donor-matched monocyte cultures as early as 24 h after cytokine addition. More noticeable morphological changes were observed by day 4 (Figure 1a, left panel). By day 5, the immature IL-15 (I'm-IL-15) DCs were firmly adhered to the plate, whereas imIL-4 DCs generated from the same donor were loosely adherent. Treatment with lipopolysaccharide (LPS) and tumor necrosis factor-α (TNFα), a conventional maturation induction procedure, for 24–48 h abated the morphological differences between the two cell types. Both LPS/TNFα-treated IL-4 (mIL-4 DCs) and IL-15 DCs (mIL-15 DCs) were strongly adherent to the dish and exhibited typical elongated dendritic protrusions (Figure 1a, right panel).

IL-15 DCs express differential levels of surface markers important to Ag presentation

Induction of Ag-specific immune responses by DCs depends on the expression of the appropriate growth factor receptors, MHC molecules and costimulatory proteins. We examined the expression of surface molecules associated with DC differentiation, maturation and immune-stimulatory function based on CD11c-gated imIL-4 DCs and mature IL-4 DCs (mIL-4 DCs) and donor-matched IL-15 DCs. First, we compared the expression levels of several markers associated with DC differentiation and maturation. imDC and mDC subsets expressed very low levels of CD14, a marker highly expressed on the precursor monocytes, which was detected on both imDC and mDC subsets at very low levels, suggesting that the precursor monocytes have undergone differentiation (Figures 1b and c). The DC-specific marker DC-SIGN (CD209) was expressed significantly less on IL-15 DCs compared with IL-4 DCs (immature, $n=7$, $P=0.02$; mature, $n=7$, $P=0.03$; Figures 1b and c). CCR7, a lymphoid migration marker, was expressed at similar levels on both imDC subsets, whereas mIL-4 DCs expressed significantly more CCR7 than mIL-15 DCs ($n=7$, $P=0.02$). The Ag presentation MHC class I molecule (HLA-I) was expressed at significantly higher levels ($n=8$, $P=0.02$) on imIL-15 DCs as compared with imIL-4 DCs, but such difference disappeared after LPS/TNFα treatment (Figures 1d and e). The MHC class II molecules (HLA-DR) were expressed at similar levels on both DC types regardless of the LPS/TNFα treatment state. The expression of CD1a, which is involved in lipid Ag presentation, was significantly lower on imIL-15 DCs and mIL-15 DCs than on IL-4 DCs ($n=9$; imDC, $n=9$; mDC, $n=7$; $P=0.004$). The expression levels of CD80 and CD83, the molecules involved in T-cell activation, was similar between the two DC subsets. However, the costimulatory molecule CD86 was expressed at higher levels on IL-4 DCs as compared with IL-15 DCs (immature, $n=6$, $P=0.03$; mature, $n=8$, $P=0.008$; Figures 1d and e). Interestingly, imIL-15 DCs expressed significantly increased amount of CD40, which is a DC and T-cell activation

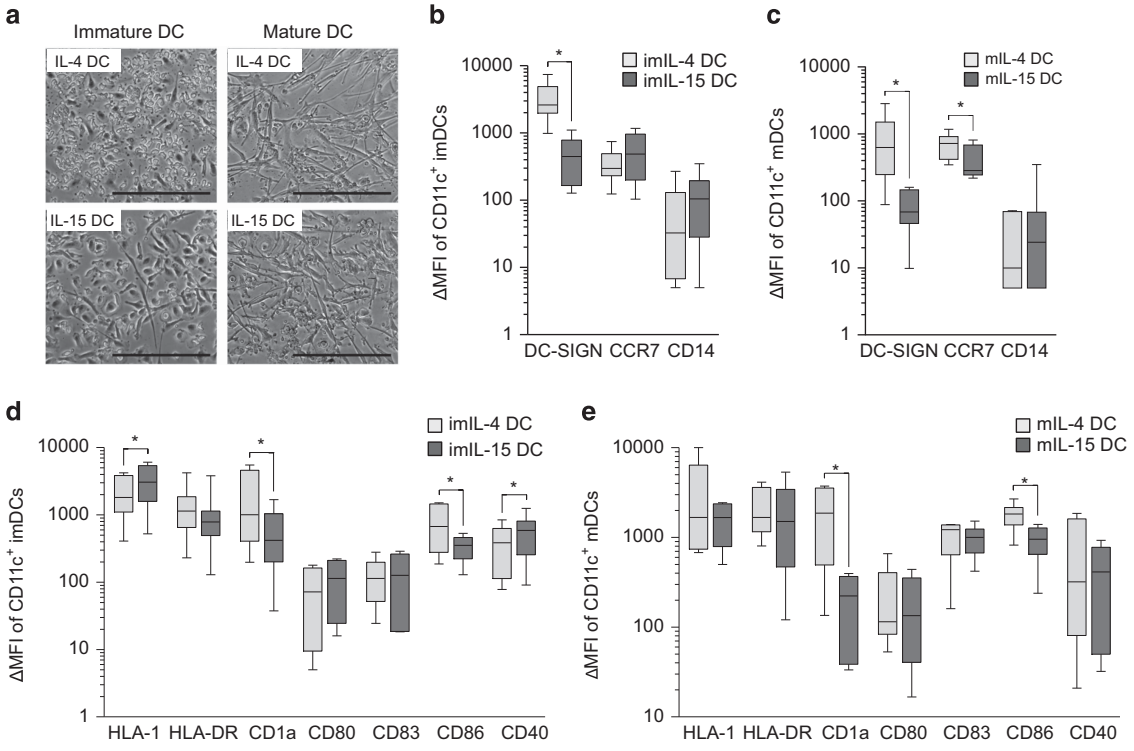

Figure 1 Morphological and surface characteristics of IL-4 and IL-15 DCs. (**a**) Representative images of adherent PBMC-derived DCs from the same donor. ImDCs were derived after differentiation for 5 days and matured for 24–36 h; the inserted bar indicates 0.1 mm. (**b**–**e**) Flow cytometry analyses of surface molecules of donor-matched IL-4 DCs and IL-15 DCs. ΔMFI after subtracting the isotype control signals were analyzed and presented, $n=5$–9. Statistical significance between the different DC types was based on Wilcoxon's matched-pairs signed-rank test with *P*-value $\leqslant 0.05$ being significant (*).

molecule, as well as a critical B-cell co-stimulatory molecule ($n=8$, $P=0.04$; Figures 1d and e).

The LPS/TNFα-treated IL-15 DCs exhibit an increased Ag uptake potential

We have previously reported that hematopoietic progenitor cell-derived imIL-15DC exhibit Ag uptake ability similar to that of IL-4 DCs.[15] Here we further assessed the abilities of LPS/TNFα-treated IL-4 DCs and IL-15 DCs to uptake and process Ags based on a fluorescein isothiocyanate (FITC)-conjugated ovalbumin (OVA-FITC) flow cytometry assay. The LPS/TNFα-treated DCs were incubated with FITC-conjugated ovalbumin (OVA-FITC) at 4 or 37 °C, and then the percentages of $CD11c^+$ cells that endocytosed OVA-FITC was determined. Although not statistically significant, on average, the LPS/TNFα-treated IL-15 DCs (mIL-15 DCs) appeared to be more efficient at internalizing OVA than the donor-matched mIL-4 DCs, as illustrated by representative flow graphs in Figure 2a, and repeats of DCs derived from three matched donors (Figure 2b).

The LPS/TNFα-treated IL-15 DCs secrete markedly increased amounts of inflammatory cytokines

In addition to presenting Ags and providing costimulation to induce T-cell responses, DCs also polarize immune responses by secreting immune-modulatory cytokines such as IL-12 and interferon-γ (IFN-γ).[16] To examine the cytokine expression profiles of the two types of DCs, we used a quantitative multiplex enzyme-linked immunosorbent assay (ELISA) array method and the Illumina expression microarray approach that detected cytokine-related gene expression (Tables 1 and 2, respectively). In comparison with mIL-4 DCs, mIL-15 DCs produced much higher levels of IL-15, which is an important factor in NK cell activation and the maintenance of CD8 T-cell population.[17,18] Furthermore, mIL-15 DCs secreted markedly greater amounts of proinflammatory cytokines, including IL-1α, IL-1β, IL-6, TNFα, TNFβ and IFN-γ, compared with mIL-4 DCs, suggesting that mIL-15 DCs are more proinflammatory than mIL-4 DCs. The latter results corroborate well with our previous finding that IL-15-driven DC progenitors from hematopoietic stem cells consistently produced more inflammatory cytokines than IL-4 DCs upon LPS/TNFα treatment.[15]

To further verify this, we evaluated RNA expression of several key inflammatory cytokines by semiquantitative RT-PCR (Figure 2c) and quantitative RT-PCR (qRT-PCR) (Figure 2d). The IFN-γ, TNFα and IL-6 transcripts were consistently expressed at higher levels at 330-, 14- and 20-folds, respectively, in donor-matched mIL-15 DCs than mIL-4 DCs (Figure 2d).

IL-15 DCs drive prominent memory and primary effector CD4 and CD8 T-cell responses

IL-15 DCs have been shown to elicit a strong antitumor CD8 T-cell response.[9,10,19] The capacity of mIL-15 DCs to prime primary as well as memory adaptive T-cell responses in relation to the classical mIL-4 DCs derived from the same donor, however, was unknown. To

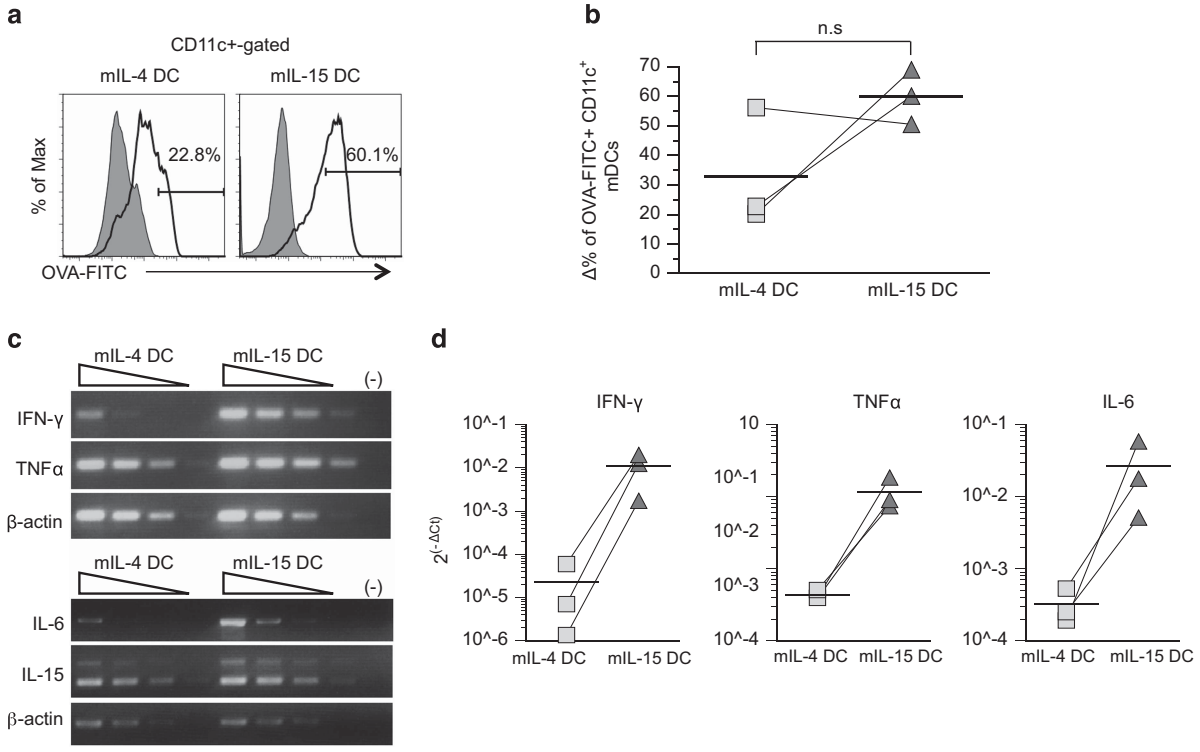

Figure 2 Increased Ag uptake function with prominent increases in inflammatory cytokine production of IL-15 DCs. (**a** and **b**) Comparison of Ag uptake functions of mIL-4 DCs versus mIL-15 DCs. mDCs were incubated with 10 μg ml^{-1} OVA-DQ for 30 min at 37 °C, or at 4 °C as control, and stained with anti-CD11c Ab and analyzed by flow cytometry. Line and shaded gray histogram graphs indicate incubation with OVA-DQ at 37 and 4 °C, respectively. The OVA uptake was calculated by subtracting the percentage of $CD11c^+$ mDCs that nonspecifically internalized OVA-DQ at 4 °C from that at 37 °C. The Δ% values of $OVA^+/CD11c^+$ mDCs from three matched donors were compared and the average percentage values were illustrated by horizontal bars. (**c**) Semiquantitative RT-PCR of IFN-γ, TNFα, IL-6, IL-15 and β-actin in mDCs. cDNA generated from RNAs pooled from three donors was serially diluted at 0, 1:10, 1:100 and 1:1000 for analysis. (**d**) Quantitative SYBR green RT-PCR of IFN-γ, TNFα and IL-6 gene levels in imDCs and mDCs. cDNAs pooled from three donors were analyzed. Relative cytokine gene expression was normalized with β-actin expression and the average percentage values illustrated by horizontal bars. Donor-paired specimens are shown by a line connection.

investigate mDC-primed memory adaptive T-cell responses, we pulsed the mDCs with a mixture of short overlapping matrix phosphoprotein 65 (pp65) peptides based on the human cytomegalovirus (CMV), a common virus that leads to chronic asymptomatic infection in the adult population, and then cocultured the DCs with autologous peripheral blood lymphocytes (PBLs) for 14–16 days as described previously.[20] The effector functions of CMV pp65-specific T cells were examined after a brief restimulation with the same subset of autologous mDCs pulsed with either the pp65 peptide mixture or an unrelated control Wilms tumor 1 peptide mixture. Ag-specific T-cell responses were then calculated by subtracting the percentage of T cells responding to the nonspecific peptide control. We found that mIL-15 DCs stimulated anti-CMV pp65 memory T-cell responses of both CD4 and CD8 T cells more efficiently than mIL-4 DCs. Specifically, the number of CD4 and CD8 T cells producing IFN-γ and/or CD107a degranulation in response to CMV pp65 was significantly greater when primed with mIL-15 DCs than with mIL-4 DCs (IFN-γ^+, CD107a$^+$ or IFN-γ^+CD107a$^+$ T cells, $n=6$; Figure 3a).

Table 1 ELISA array analysis of cytokine expression profiles of LPS/TNFα-treated IL-4 and IL-15 DCs

Cytokine	*Donor A (pg ml^{-1})*		*Donor B (pg ml^{-1})*	
	mIL-4 DC	*mIL-15 DC*	*mIL-4 DC*	*mIL-15 DC*
IL-1a	135 ± 5.3	332 ± 30.1	32 ± 0.4	1228 ± 37
IL-1b	338 ± 28	601 ± 54	92 ± 3.2	2696 ± 90
IL-4	3 ± 0.5	4 ± 0.1	3 ± 0.3	2 ± 0.3
IL-12p70	6 ± 0.3	16 ± 1.5	2 ± 0.3	25 ± 2.1
IL-15	25 ± 3.5	2358 ± 147	23 ± 2.2	248 ± 27
IFN-γ	<1	2332 ± 185	<1	1905 ± 35
IL-6	652 ± 56	1664 ± 34	52 ± 2.3	8036 ± 311
TNFα	149 ± 16	1438 ± 41	72 ± 2.5	3152 ± 104

Abbreviations: DC, dendritic cells; ELISA, enzyme-linked immunosorbent assay; IFN, interferon; IL, interleukin; LPS, lipopolysaccharide; TNFα, tumor necrosis factor-α.

In addition to the anti-CMV pp65 T-cell responses, we also examined the ratio of different effector and memory CD4 and CD8 T-cell subsets in the cocultures after stimulation with CMV pp65-pulsed mDCs. We analyzed the different T-cell subsets based on a series of surface markers associated with central memory: CD45RA$^-$ CD27$^+$ CD28$^+$ CD62L$^+$ CCR7$^+$; effector memory: CD45RA$^-$ CD27$^+$ CD28$^+$ CD62L$^-$ CCR7$^-$; and terminal effector (Teff): CD45RA$^{+/-}$ CD27$^-$ CD28$^-$ CD62L$^-$ CCR7$^-$ T cells.[20] Multicolor flow cytometry analyses indicated that the different T-cell subsets were equally activated by both types of DCs. The results showed that mIL-15 DCs consistently generated more CD4 and CD8 Teff cells compared with mIL-4 DCs; however, the differences were not statistically significant upon analysis of several matched donors ($n=6$, $P=0.09$; Figure 3b). On the other hand, IL-4 DC stimulation led to a significantly greater number of CD4 and CD8 central memory cells than the donor-matched IL-15 DCs ($n=6$, $P=0.03$; Figure 3b).

Besides CMV pp65-specific memory T-cell responses, we also evaluated the ability of IL-15 DCs to initiate primary immune responses against a pool of overlapping hepatitis C virus (HCV) core protein peptides. mDCs from healthy donors of HCV-negative status were pulsed with HCV core synthetic peptides, and then cocultured with autologous T lymphocytes. Despite the much lower number of T cells that responded to HCV core compared with the memory responses against CMV pp65, stimulation by mIL-15 DCs significantly promoted the production of IFN-γ and/or CD107a degranulation in CD4 and CD8 T cells as compared with mIL-4 DCs-stimulated T cells (Figure 4a). Analyses of the central memory, effector memory and Teff subset ratios indicated that coculture with HCV core-pulsed mIL-15 DCs tended to increase the CD4 and CD8 Teff cell populations and reduce the central memory populations as compared with IL-4 DCs (Figure 4b).

IL-15 DCs promote NK cell cytolytic functions

In the primary and memory T-cell activation assays, we noticed evident differences in the expansion and functions of NK cells (CD3$^-$ CD56$^+$) in the DC-PBL cocultures. Although the expansion of NK

Table 2 Cytokine-related gene expression array analysis of LPS/TNFα-treated IL-4 and IL-15 DCs

Symbol	*Gene name*	*Accession no.*	*Probe signal*		*Fold change (mIL-15 DC vs mIL-4 DC)*
			mIL-4 DC	*mIL-15 DC*	
IL-1b	*Interleukin 1, beta*	NM_000576.2	332.9	2855.9	8.58
IL-6	*Interleukin 6*	NM_000600.1	82.5	130.8	1.59
IL-8	*Interleukin 8*	NM_000584.1	562.4	11602.9	20.63
IL-10	*Interleukin 10*	NM_000563.1	11.7	4.8	−2.43
IL-12A	*Interleukin 12a (p35)*	NM_000882.2	9.3	8.5	−1.09
IL-12B	*Interleukin 12b (p40)*	NM_002187.2	38.5	2.6	−14.81
TNFα	*Tumor necrosis factor*	NM_000594.2	537.1	721.9	1.34
TNFSF10	*TRAIL*	NM_003810.3	19.7	178.8	9.08
IL-15	*Interleukin 15 (SSP isoform)*	NM_000585.2	479.7	156.1	−3.07
IL-15	*Interleukin 15 (LSP isoform)*	NM_172175.1	40.7	12.5	−3.26
CCL1	*Chemokine C–C motif ligand 1 (i-309)*	NM_002981.2	163.1	369.3	2.26
CCL3	*Chemokine C–C motif ligand 1 (mip-1a)*	NM_002983.2	2080.2	9689.6	4.66
CCL7	*Chemokine C–C motif ligand 7 (MCP3)*	NM_006273,3	60.7	575.1	9.47
CXCL10	*IP-10, IFN-γ-induced protein 10*	NM_001565.3	258.2	1341.9	5.20
TLR1	*Toll-like receptor 1 (TIL)*	NM_003263.3	7.7	150	19.48
TLR2	*Toll-like receptor 2 (TIL4)*	NM_003264.3	184.9	1520.5	8.22

Abbreviations: DC, dendritic cells; IL, interleukin; LPS, lipopolysaccharide; TNFα, tumor necrosis factor-α.

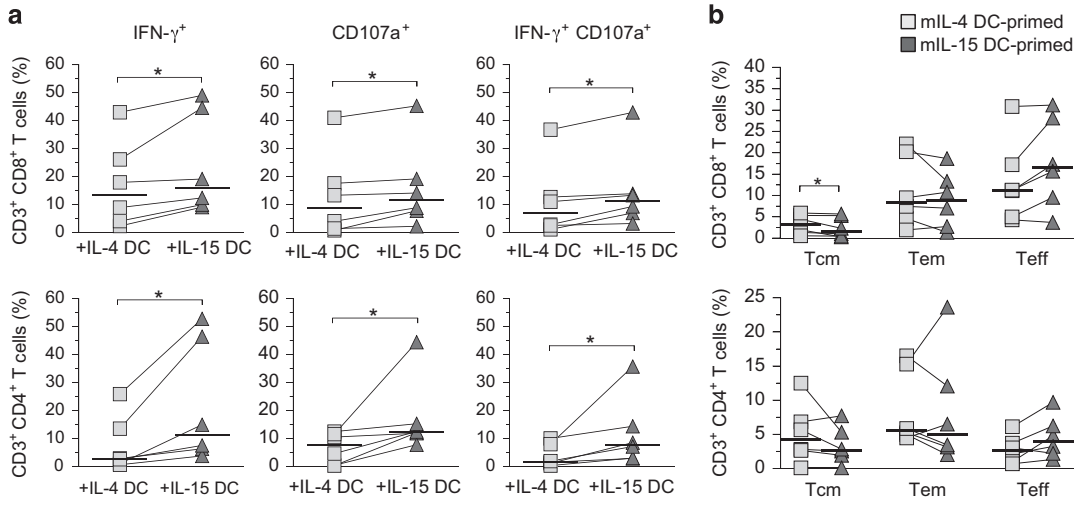

Figure 3 Increased CMV-specific CD4 and CD8 T-cell recall responses induced by IL-15 DCs. (**a**) Analyses of Ag-specific effector activities of memory T cells against CMV pp65. mDCs were pulsed with CMV pp65 pooled peptides and incubated with autologous T cells for 16 days. The percentages of specific responding effector T cells producing IFN-γ and CD107a are presented based on results of intracellular staining and flow cytometry. Donor-paired T-cell responses after IL-4 DC (gray squares) versus IL-15 DC stimulation (dark triangles) are depicted by the lines connecting the squares to triangles. Median responding T-cell percentages are indicated by the horizontal bars and statistically significant differences (*) determined by two-tailed, Wilcoxon's matched-pairs signed-rank test with *P*-value $\leqslant 0.05$ ($n=6$) are shown. (**b**) Analysis of memory and effector CD4 and CD8 T-cell population distribution in a CMV pp65-primed PBL recall Ag stimulation assay. Central memory (Tcm), effector memory (Tem) and Teff T cells were identified based on characteristics of surface markers, CD45RA, CD27, CD28, CD62L and CCR7, in addition to CD3, CD4 and CD8 by flow cytometry as described previously.[20] Donor-paired T-cell responses after IL-4 DC- (gray squares) vs IL-15 DC stimulation (dark triangles) are depicted by the lines connecting the squares to triangles. Median responding T-cell percentages are indicated by the horizontal bars and statistically significant differences (*, $n=6$) are shown ($n=6$).

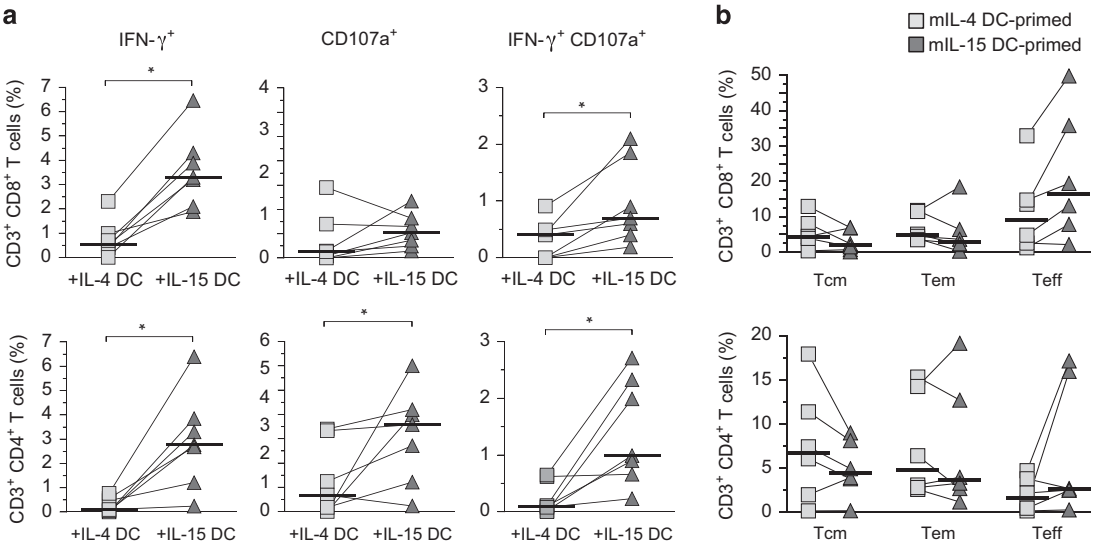

Figure 4 Increased HCV-specific CD4 and CD8 primary T-cell responses induced by IL-15 DCs. (**a**) Analyses of Ag-specific effector activities of memory T cells against HCV core protein. mDCs were pulsed with HCV core pooled peptides and incubated with autologous T cells for 16 days. The percentages of specific responding effector T cells producing IFN-γ and CD107a are presented based on the results of intracellular staining and flow cytometry. Donor-paired primary T-cell responses after IL-4 DC (gray squares) versus IL-15 DC stimulation (dark triangles) responses are depicted by the lines connecting the squares to triangles. Median HCV core-responding T-cell percentages are indicated by the horizontal bars and statistically significant differences determined by two-tailed, Wilcoxon's matched-pairs signed-rank test with *P*–value $\leqslant 0.05$ ($n=6$) are shown. (**b**) Analysis of memory and effector CD4 and CD8 T-cell population distribution after recall Ag stimulation in HCV core-primed PBLs. Central memory (Tcm), effector memory (Tem) and Teff cells were identified based on group of surface markers by flow cytometry as described here. Donor-paired primary T-cell responses after IL-4 DC (gray squares) versus IL-15 DC stimulation (dark triangles) are depicted by the lines connecting the squares to triangles. Median HCV core-responding T-cell percentages are indicated by the horizontal bars ($n=6$).

cells in either the IL-4-DC- or IL-15-DC-primed memory or primary T-cell cocultures was not significantly different with matched donor cells (Figures 5a and b: CMV pp65 DC cocultures and Figures 5d and e: HCV core DC cocultures), the functionality of the NK cells appeared more activated by IL-15 DCs than IL-4 DCs. To examine the cytolytic activities of the NK cells in the cocultures, the NK-sensitive K562 cells were labeled with carboxyfluorescein succinimidyl ester and mixed with the cocultured cells at a serial range of

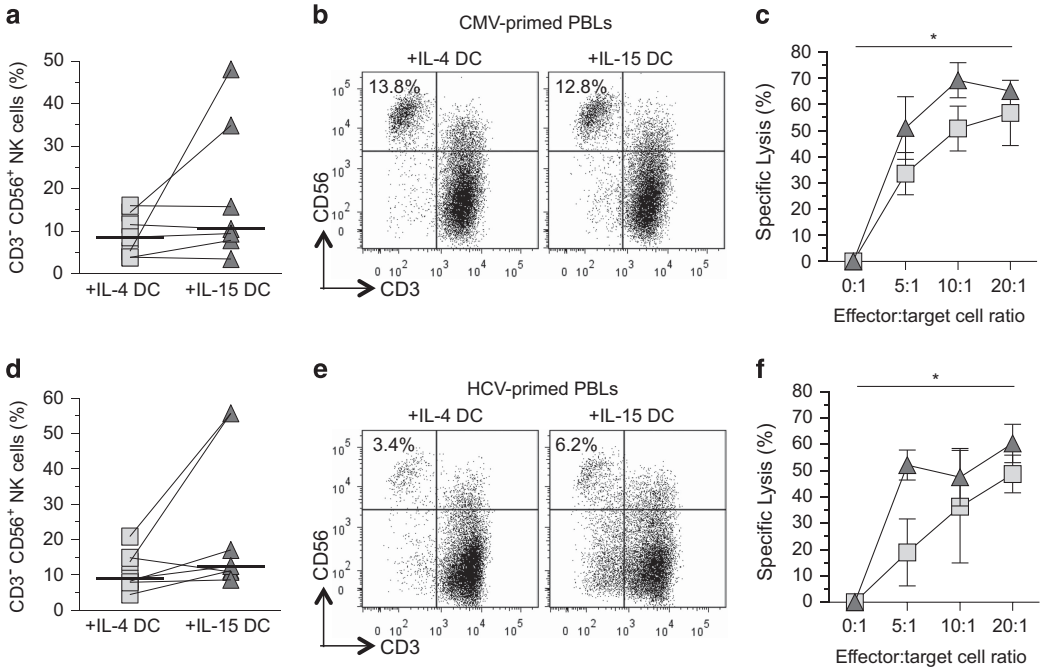

Figure 5 Analyses of expansion and cytolytic activities of NK cells in the DC cocultures. (**a** and **d**) Percentage of NK cells ($CD3^-$ $CD56^{\pm}$) within the autologous PBLs. The PBLs had been cocultured for 14–16 days with mIL-4 DCs or donor-matched mIL-15 DCs pulsed with CMV pp65 peptides or HCV core peptides. Differences in the median percentages of NK cells were determined to be statistically insignificant between the mIL-4 DC- and mIL-15 DC-primed lymphocytes using Wilcoxon's matched-pairs signed-rank test in which the *P*-value $\leqslant 0.05$ was considered significant. (**b** and **e**) Representative flow cytometry dot plots from one of the donors showing the expanded T cells ($CD3^+$) and NK cells ($CD3^-$, $CD56^+$) in the autologous PBLs cocultured with donor-matched mIL-4 DCs or mIL-15 DCs after incubation with CMV or HCV peptide-pulsed mIL-4 DCs or mIL-15 DCs. The percentages of the NK cells in PBLs stimulated with the CMV pp65 or the HCV core peptides for this particular donor are indicated. (**c** and **f**) Donor-matched, NK cell-specific lysis of CSFE-labeled K562 target cells. The effector-to-target cell ratio variables were evaluated in triplicate and the mean percentage ± s.d. is shown. The light squares and dark triangles represent cells cocultured with mIL-4 DCs and mIL-15 DCs, respectively, $N=2$. The representative result of two independent experiments evaluating two donors is shown. Statistical significance was determined using paired two-way analysis of variance (ANOVA) with Bonferroni *post hoc* tests with *P*-value $\leqslant 0.05$ being significant (*).

effector-to-target cell ratios for 5 h and analyzed. Before analysis, a constant amount of APC styrene beads were added to each sample. The cell lysis data were obtained based on the collection of 3000 APC beads. The result demonstrated that after exposure to DCs pulsed with either CMV or HCV peptides, the NK cells from the IL-15 DC cocultures displayed increased cytolytic activities (Figures 5c and f). These results demonstrate that both innate and adaptive immune responses can be effectively activated by IL-15 DCs.

IL-15 activates distinct STAT and MAPK signaling pathways in DCs

The molecular signaling downstream of IL-4 and IL-15 has been studied primarily in lymphocytes in which IL-4 primarily induces STAT6 and ERK1/2 (extracellular signal-regulated kinase 1/2) MAPK phosphorylation and IL-15 predominantly activates STAT5.[13,14,21] In some other cell types, IL-4 can also activate p38 MAPK, and IL-15 has been shown to induce phosphorylation of STAT3 or p38 MAPK.[22–24] The intracellular signaling regulated by GM-CSF and IL-4 or IL-15 in DCs, however, has not been well characterized. To understand how IL-4 and IL-15 polarize DCs, we first analyzed the expression of IL-4 receptor α (IL-4Rα) and IL-15 receptor α (IL-15Rα). We found that IL-4Rα and IL-15Rα were similarly expressed on both imIL-4 and imIL-15 DCs and mIL-4 and mIL-15 DCs, suggesting that both DC types can respond to IL-4 and IL-15 (for further details see Supplementary Figure S1).

To investigate cytokine-mediated intracellular signaling, we examined the activities of STAT3, STAT5, STAT6, ERK1/2 MAPK and p38 MAPK pathways in CD11c-gated imIL-4 and imIL-15 DCs and mIL-4 and mIL-15 DCs based on phosphoprotein flow cytometry, and representative flow cytometry results are illustrated in Figures 6a (imDcs) and b (mDCs). As expected, activated STAT6 levels were significantly increased in IL-4 DCs as compared with IL-15 DCs after quantitative analysis of phosphorylated STAT6 (pSTAT6), supported both by the expression intensity (variations of mean fluorescence index (ΔMFI); Figures 5c and d: imDC, $n=6$, $P=0.03$; mDC, $n=9$, $P=0.01$) and the total cell population (ΔMFI percentage; Figures 5e and f: imDC, $n=6$, $P=0.03$; mDC, $n=9$, $P=0.03$). Furthermore, the phosphorylated ERK1/2 MAPK (pERK1/2) levels were significantly higher in mIL-4 DCs compared with mIL-15 DCs, consistent both for the ΔMFI and Δpercentage (pERK1/2: imDC, $n=5$, $P=0.06$; mDC, $n=7$, $P=0.02$; Figures 5d and f). Surprisingly, the STAT5, which is the canonical signaling pathway for IL-15 in lymphocytes, was significantly more activated in imIL-4DC and mIL-4 DCs than in the IL-15 DCs (Figures 5c and e: ΔMFI—imDC, $n=12$, $P=0.0005$; mDC, $n=10$, $P=0.03$; Figures 5d and f: Δpercentage—imDC, $n=12$, $P=0.0005$; mDC, $n=10$, $P=0.02$).

We detected similar expression of pSTAT3 ($n=6$) and phosphorylated p38 (pp38) ($n=5$) in imIL-4 DCs and imIL-15 DCs (Figures 5c and e). However, pSTAT3 and pp38 were both elevated in mIL-15 DCs when compared with mIL-4 DCs, as illustrated by both MFI and cell percentage (Figure 5d: ΔMFI—pSTAT3, 18 vs 125, $n=8$, $P=0.008$; pp38, 18 vs 83, $n=7$, $P=0.02$; Figure 5f: Δpercentage—pSTAT3, $P=0.02$; pp38, $P=0.02$). The expression microarray analysis of STAT3-, STAT5- and STAT6-responsive genes in mIL-4 DCs and mIL-15 DCs corroborated these findings (Supplementary Table S1).

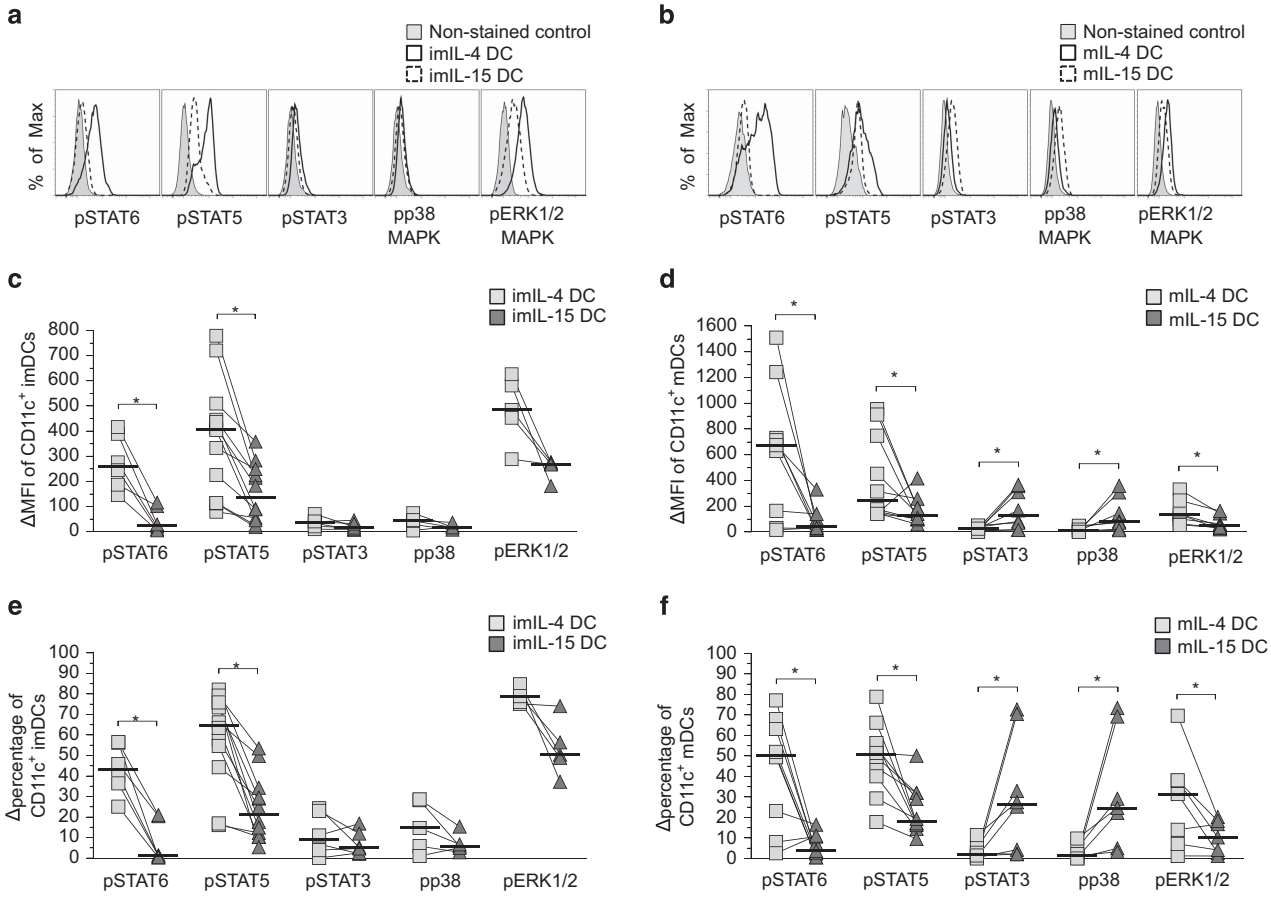

Figure 6 Analyses of IL-4 and IL-15 signaling profiles in imDCs and mDCs. (**a** and **b**) Representative phospho-STAT and phospho-MAPK flow cytometry histograms for CD11c$^{\pm}$-gated imIL-4 and imIL-15 DCs (**a**) and (**b**) mIL-4 and mIL-15 DCs from a single donor. The imDCs are indicated by solid lines, whereas mDCs are shown as dashed lines. The non-stained controls are shown by the shaded areas consisted of a mixture of both DC types. (**c**–**f**) Cytokine-induced signaling profiles in DCs. The ΔMFI and Δpercentage of phosphoprotein-positive, CD11c^{+}-gated, immature (**c** and **e**) and mature (**d** and **f**) donor-matched IL-4 DCs (gray squares) and IL-15 DCs (dark triangles) were normalized with control non-stained cells. Bar indicates the median value. Statistical significance was determined by Wilcoxon's matched-pairs signed-rank test with P-value $\leqslant 0.05$ being significant (*), $n = 7$–10.

Therefore, the treatment with LPS/TNFα appears to trigger a distinct signaling profile in IL-15 DCs.

STAT3, but not p38 MAPK, signaling has a central role in IFN-γ production in IL-15 DCs

The above results showed that increased STAT3 and p38 MAPK activities in IL-15 DCs was associated with LPS/TNFα treatment and was unique to IL-15 DCs. To further determine the role of these signaling pathways in driving IL-15 DC functions, we applied specific inhibitors to target these two pathways and quantified cytokine expression by intracellular antibody (Ab) staining and flow cytometry. IL-15 DCs were treated with TNFα/LPS for 24 h, washed thoroughly and cultured with either p38 MAPK inhibitor (SB203580) or STAT3 inhibitor (stattic) in the presence of Golgi blocker brefeldin A for 6 h. The levels of intracellular IFN-γ and TNFα were assessed in CD11c-gated cell population. The concentrations of inhibitors had been first optimized using THP-1 cells and peripheral blood mononuclear cells (PBMCs) (not shown). We found that inhibition of p38 MAPK or STAT3 signaling did not affect the expression of TNFα in mIL-15 DCs (Figures 7a and b). Similarly, inhibition of p38 MAPK did not significantly affect IFN-γ expression in mIL-15 DCs (Figures 6c and d). In contrast, the expression of IFN-γ was significantly decreased in mIL-15 DCs upon inhibition of the STAT3 signaling pathway (Figures 7c and d: ΔMFI, $n = 8$, $P = 0.04$; and changes in cell percentage, $P = 0.02$).

DISCUSSION

In this study, we characterized the differential molecular signaling between IL-4 and IL-15 DCs. Our results demonstrate that besides differences in physical features and immune-stimulatory abilities of the two lineages of DCs, intracellular signaling through STAT3 and p38 MAPK activations contributes to the high immune effector activities of the LPS/TNFα-treated IL-15 DCs.

The morphological feature of IL-15 DCs in this study differs somewhat from the previously characterized IL-15 DCs.[7] We observed that during induction of IL-15 DCs, the adherent monocytes gradually became enlarged and displayed fibroblast-like morphology by day 5. In contrast, when cultured in IL-4, the monocytes gradually became floating enlarged cells with small dendrites resembling typical DCs. Such morphological differences were consistently observed in DCs derived from numerous donors ($n > 10$). The plausible explanations to the observed differences with the IL-15 DCs include: (1) different treatment conditions: instead of low levels of LPS (10 ng ml^{-1}), we used both LPS (1 μg ml^{-1}) and TNFα (50 ng ml^{-1}) for the activation of DCs, and (2) different treatment time for monocytes: instead of treating monocytes with cytokines for 3 days and activating with LPS

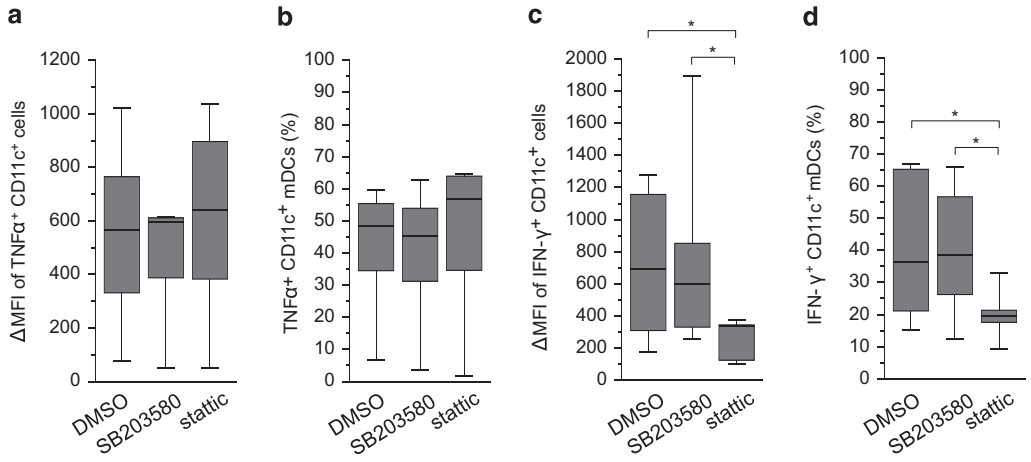

Figure 7 Correlation of STAT3 signaling with the expression of IFN-γ but not TNFα in IL-15 DCs. $CD11c^+$ mIL-15 DCs were treated with control dimethyl sulfoxide (DMSO), or specific inhibitors targeting p38 MAPK (SB203580) and STAT3 (stattic) signaling pathways as indicated, and stained with phosphoprotein-specific Abs and analyzed by flow cytometry. (**a** and **b**) Intracellular staining for TNFα and (**c** and **d**) intracellular staining for IFN-γ expression. Bars in the center indicate median values of the compiled staining results. Statistical significance was determined by Wilcoxon's matched-pairs signed-rank test with *P*-value $\leqslant 0.05$ being significant (*); $n=6$ for TNFα and $n=7$ for IFN-γ.

for 2 days, we treated monocytes with cytokines for 5 days, and then activated (matured) for 24 h.

Interestingly, IL-15 DCs exhibited several phenotypically distinct characteristics from their donor-matched IL-4 DC counterparts. In contrast to IL-4 DCs, IL-15 DCs expressed significantly less of the DC-related molecule DC-SIGN (CD209). As for biological relevance, DC-SIGN binds the HIV-1 envelope glycoprotein gp120 to facilitate infection of other sensitive cell types ($CD4^+$ $CCR5^+$ or $CXCR4^+$) *in trans*. Thus, IL-15 DCs with relatively decreased DC-SIGN may be less likely to promote HIV infection. The imIL-15 DCs expressed higher amounts of HLA class I and the costimulatory molecule CD40 compared with imIL-4 DCs, which suggests that even at an immature state (i.e. not treated with TNFα and LPS), IL-15 DCs may have immunostimulatory capabilities. Interestingly, in relation to mIL-4 DCs, donor-matched mIL-15 DCs seem to be more phenotypically 'immature' with significantly less CCR7, a key DC maturation marker that mediates DC migration toward lymph nodes.

The results from the flow cytometry analyses of surface markers and costimulatory receptors, together with the data of cytokine/chemokine ELISA array, demonstrate that IL-15 DCs display high signal 3 (secreted immune modulators) but low signal 1 (MHC molecules and CD1a), signal 2 (T-cell costimulators, e.g. CD40, CD80, CD86, PD-L1, ICAM-1), DC-related molecule (DC-SIGN, DC-LAMP) and migration marker CCR7. Consistent with this observation, IL-15 DCs secreted increased amounts of proinflammatory cytokines and increased levels of T-cell differentiation factors, many of which were expressed at several orders of magnitude higher than IL-4 DCs (Tables 1 and 2 and Figure 2), which is in agreement with the characteristics of previously described stem-cell-derived IL-15 DCs.[15] IL-15 DCs produce high levels of chemokines such as MCP-1, IL-8, RANTES and eotaxin, which can induce the migration of monocytes and other immune cells such as NK and dendritic cells, and are known to recruit naive T cells, monocytes, neutrophils and other innate immune cells. Thus, we speculate that *in vivo*, IL-15 DCs could primarily be residential Ag-presenting cells with high innate immune effector functions. This is further supported by the increased NK cell cytolytic activities after IL-15 DC stimulation (Figure 5).

Although IL-15 is known to induce STAT5 signaling in lymphocytes and other cell types, we did not observe such activities in IL-15 DCs; no pSTAT5 activation or upregulation was detected in either imIL-15DCs or mIL-15 DCs. The activation of STAT5 has been shown to maintain and prolong surface expression of costimulatory molecules such as CD40, CD80, CD86, CD83 and HLA-DR, and promotes a Th2, rather than Th1, response in DCs.[25] This is consistent with the observation that some of the costimulatory molecules were detected at higher levels in IL-4 DCs than in IL-15 DCs (Figure 1 and data not shown). GM-CSF is known to activate both the STAT5 and ERK1/2 pathways.[26] We found that GM-CSF receptor (GM-CSFR) was expressed at significantly higher levels on imIL-15 compared with imIL-4 DCs (data not shown). Although this trend was switched after DC maturation in which mIL-4 expressed more GM-CSFR than mIL-15, the dearth of pSTAT5 in imIL-15 and mIL-15 DCs could not be due to the lack of GM-CSFR expression.

In lymphocytes, IL-15 binds to its specific receptor subunit IL-15Ra, which then trimerizes with the IL-2Rβ and γC dimer and leads to the phosphorylation and activation of the STAT5 pathway (pSTAT5).[13,14] In some cell types, IL-4 and IL-15 have been shown to activate alternative STAT and/or MAPK signaling pathways in addition to their respective canonical STAT pathway in lymphocytes. IL-4 has been shown to phosphorylate and activate the ERK1/2 (pERK) or p38 (pp38) pathways, whereas IL-15 stimulation may phosphorylate and activate the STAT3 (pSTAT3), p38 and/or ERK1/2 pathways.[21–24,27] Despite their importance in modulating immune responses, these signaling pathways have not been characterized in human DCs. We found that IL-15 DCs exhibited much less activated STAT5, STAT6 and ERK1/2 than donor-matched IL-4 DCs, whereas STAT3 and p38 pathways were significantly more activated upon LPS/TNFα treatment of IL-15 DCs. STAT3 activity negatively affects maturation and subsequent immune functions of DCs in several murine-based studies.[28,29] Conversely, activation of the p38 MAPK is thought to promote DC maturation and their immune-stimulatory abilities.[30] Our results suggest that STAT3 and p38 signaling pathways have a lineage-specific role in modulating mIL-15 DC functions. The latter could be a result of a high steady-state amount of IL-6 produced by IL-15 DCs, followed with marked upregulation of IL-6 upon maturation (Tables 1 and 2). IL-6 has been reported to induce transient activation of STAT3,[31] and our data indicate a tight association of STAT3 signaling with IFN-γ but not TNFα production in IL-15 DCs

(Figure 7). Therefore, for the first time, we have presented clear evidence of correlation of IL-6 with IFN-γ effector activities in DCs through STAT3 regulation. Although STAT3 signaling has been reported to be a key checkpoint in fms-like tyrosine kinase-3 ligand-regulated DC development during hematopoietic progenitor cell differentiation, it also has an intrinsic negative regulatory role through IL-10 and IL-6 signaling in DCs in mice.[29,32,33] Our study indicates that the same STAT3 signaling pathway may be involved in both positive and negative immune effector regulation in DCs. The detailed signaling network characterized for DCs in this study helps draw a clear picture of the immune effector role of IL-15 DCs implicated in immunotherapy and in *in vivo* settings.

The compiled results support that DCs differentiated under IL-15 signaling not only promotes a strong adaptive immune response but also a strong innate immune effector response. Different from the IL-15-induced STAT5 activation pathway in lymphocytes and other immune cells, IL-15 does not directly facilitate STAT5 phosphorylation in DCs. Instead, increased p38 MAPK and STAT3 activities in IL-15 DCs corroborate the release of IFN-γ and contribute to their strong immune effector activities.

METHODS

Blood donors

Buffy coats from anonymous healthy donors were purchased from LifeSouth Civitan Blood Center (Gainesville, FL, USA) with approval from the Institutional Review Board (IRB-01) of University of Florida.

Generation of adherent PBMC-derived IL-4 and IL-15 DCs

PBMCs from healthy donors were isolated from buffy coats by gradient density centrifugation in Ficoll-Hypaque (GE Healthcare Bio-Sciences AB, Piscataway, NJ, USA) as described previously.[34] DCs were prepared as described previously,[35] with the following modifications: on day 0, the PBMCs were incubated at 37 °C for 2 h to obtain adherent monocytes, which were cultured in AIM-V medium (Invitrogen, San Diego, CA, USA). On day 1, one-half of the AIM-V medium was supplemented with 50 ng ml^{-1} GM-CSF (BioSource, Invitrogen Inc., Carlsbad, CA, USA) and either 25 ng ml^{-1} IL-4 (BioSource) to generate IL-4 DCs or 100 ng ml^{-1} IL-15 (Gentaur Molecular, Brussels, Belgium) to generate IL-15 DCs. On day 3, fresh AIM-V media containing the same final concentration of cytokines was added. After 5 days, imDCs were harvested using 10 mM EDTA-PBS (Sigma-Aldrich, St Louis, MO, USA) and a cell lifter. imDCs were either cryogenically stored or further cultured with maturation factors, TNFα (50 ng ml^{-1}; Gentaur) and LPS (1 μg ml^{-1}; Sigma-Aldrich), for 24 h to obtain mDCs. The term 'maturation' for IL-15 DCs refers TNFα and LPS treatment based on conventional terminology used for IL-4 DCs without prejudice. The phenotype of imDCs and mDCs were analyzed with fluorochrome-conjugated Abs specific for DC-related surface markers.

Monoclonal Abs and inhibitors

Fluorochrome-conjugated monoclonal Abs against human CD11c (clone B-ly6, PE or APC), CD25/IL-4Rα (clone hIL4R-M57, PE), CD137L/4-1BBL (clone C65-485, PE), CD1a (clone HI149, APC), CD40 (clone 5C3, APC), IFN-γ (clone B27, APC), CD86 (clone FUN-1, FITC), CD45RA (clone HI100, FITC), CD107a/LAMP-1 (clone H4A3, FITC), CD14 (clone M5E2, pacific blue), CD3 (clone UCHT1, pacific blue), CD16 (clone 3G8, pacific blue), CD8 (clone SK1, APC-Cy7), CD80 (clone L307.4, CyC), CCR7 (clone 3D12, PE-Cy7) and CD56 (clone B159, PE-Cy7) were purchased from BD Biosciences (San Diego, CA, USA), and against CD11c (clone BU15, FITC), HLA-DR (clone TÜ36, FITC), HLA class I (clone TÜ149, FITC), CD14 (clone TÜK4, FITC), CD3 (clone S4.1, FITC), CD83 (clone HB15e, APC), CD4 (clone S3.5, PE-TexasRed), CD8 (clone 3B5, Alexa700) and TNFα (clone MP9-20A4, APC) were obtained from Caltag, Invitrogen Inc. (Carlsbad, CA, USA). Abs against CD11c (clone 3.9, PE-Cy7), PD-L1 (clone MIH1, PE-Cy7), IL-15Rα (clone eBioJM7A4, FITC), TLR4 (clone HTA125, PE), CD27 (clone M-T271, APC), DC-SIGN/CD209 (clone eB-h209, APC) and CD28 (clone O323, APC-Alexa750) were purchased from eBioscience (San Diego, CA, USA). Abs against the phosphorylated proteins STAT3 pY705 (clone 4/P-STAT3, pacific blue), STAT5 pY694 (clone 47/STAT5, Alexa488), STAT6 pY641 (clone 18/STAT6, Alexa647), p38 MAPK pT180/pY18 (clone 36/p38, pacific blue), ERK1/2 pT202/pY204 (clone 20A, Alexa647), GM-CSFR/CD116 (clone M5D12, FITC) and CD25/IL-4Rα (clone hIL4R-M57, PE) were from BD. Anti-IL-15Rα Ab (clone eBioJM7A4, FITC) was purchased from eBioscience and anti-IL-15 Ab (clone 34559, PE) was obtained from R&D Systems (Minneapolis, MN, USA). The inhibitors for p38 MAPK (SB203580) and STAT3 (stattic) were purchased from Tocris Bioscience (R&D Systems Inc., Minneapolis, MN, USA).

Synthetic pentadecapeptide pools

Human CMV matrix pp65, HCV core and Wilms tumor 1 protein peptide mixtures were obtained from JPT Peptide Technologies Inc. (Acton, MA, USA). Each peptide mixture consisted of over a hundred 15-mer synthetic peptides with 11 amino-acid overlaps across the entire length of the particular protein.

Ag uptake assay

mDCs were incubated with 10 μg ml^{-1} OVA-FITC (Molecular Probes, Life Technologies, Grand Island, NY, USA) for 30 min at 37 °C. Controls were incubated on ice for 30 min with the same concentration of OVA-FITC. DCs were washed and stained with anti-CD11c Ab. The cells were collected with the BD LSRII or the BD Caliber flow cytometer (BD Biosciences). Data were analyzed with FlowJo software (Ashland, OR, USA). When only three donors were evaluated, statistical significance was evaluated by paired, two-tailed *t*-test with *P*-values $\leqslant 0.05$ being significant.

Multiplex cytokine ELISA array

mDCs were seeded in 24-well plate in AIM-V media not containing any exogenous cytokines at a density of 1×10^6 mDCs per ml. After 24 h, the supernatants were collected and frozen. Frozen supernatants were sent to Quansys Biosciences (Logan, UT, USA) for their modified multiplex ELISA array service. Each cytokine analyst was analyzed in triplicate.

Expression microarray analysis

RNA samples were harvested from adherent PBMC-derived IL-4 and IL-15 DCs and analyzed using Illumina Human RefSeq-8 Expression BeadChips (Illumina, San Diego, CA, USA). The RNA quantity was determined with the Agilent RNA 6000 Nano Kit and Bioanalyzer (Agilent Technologies Inc., Santa Clara, CA, USA). The synthesis of double-stranded cDNA and *in vitro* transcription were performed with the Ambion Illumina Total Prep Kit (Illumina) according to the manufacturer's instructions. For each sample, input quantity for the first strand synthesis was normalized to 200 ng. After *in vitro* transcription reaction, yield of purified cRNA was assessed with the RiboGreen assay and the quality was assessed with the Agilent Bioanalyzer. BeadChip hybridization, staining and scanning were performed according to Illumina whole genome expression for BeadStation. For each sample, input of cRNA was normalized to 1500 ng. As a control, Stratagene Universal Human Reference (SUHR) RNA was labeled with the Ambion Total Prep Kit. The labeled cRNA was used as interchip hybridization replicates and showed strong correlation. Biological replicate pairs were analyzed, and for unnormalized data, the linear r^2 was >0.94 for all replicates.

Ag presentation of DCs and activation of Ag-specific T cells

mIL-4 DCs and mIL-15 DCs were loaded with 1 μg ml^{-1} β-microglobulin along with either 1 μg ml^{-1} CMV pp65 or 5 μg ml^{-1} HCV core peptide mixtures in AIM-V media for 2–4 h at 37 °C. The peptide-pulsed mDCs were irradiated for 2000 rad, washed and mixed with autologous non-adherent PBMCs at a ratio of 1:20 (DC to non-adherent PBMCs) per well in a 96-well U-bottom plate in AIM-V supplemented with 5% human AB serum. After 3 days, half of the media in the wells was replaced with complete AIM-V media containing 5% human AB serum supplemented with the final concentrations of cytokines: 12.5 U ml^{-1} IL-2, 5 ng ml^{-1} IL-7 and 20 ng ml^{-1} IL-15 (Gentaur). One-half of the media was replenished with fresh complete AIM-V containing serum and cytokines every 2 days. T-cell immune responses against CMV pp65 and HCV core proteins were analyzed on days 14–16 of the coculture using a

series of Ag recall assays. T- and NK-cell functional subsets were distinguished from the general cocultured cell population based on specific surface marker phenotypes on day 15 of the coculture by flow cytometry.

T-cell Ag recall assay

After Ag-pulsed mDC and autologous lymphocytes were cocultured for 14–16 days, the T cells were restimulated with the appropriate type of mDC generated from the same donor that had been pulsed with the original viral Ag (specific) or the control Wilms tumor 1 tumor Ag (nonspecific) peptides to determine Ag-specific induction of IFN-γ and degranulation of CD107a in T cells. The T cells were restimulated by peptide-loaded autologous mDCs at the same 1:20 mDC to lymphocyte ratio in a U-bottom plate for 5 h at 37 °C. Anti-CD107a Ab was added from the beginning. After 1 h, 6 μg ml^{-1} monensin A (Sigma-Aldrich, St Louis, MI, USA) was added and then the cells were incubated for the remaining 4 h. Cells were stained with antibodies against CD3, CD4 and CD8, fixed, permeabilized and stained with anti-IFN-γ Ab before flow cytometry analysis. Ag-specific effector functions (IFN-γ and CD107a) were evaluated by subtracting the percentage of $CD3^+$ T cells responding to the Wilms tumor 1 peptides from those reacting to the original peptides. Statistical significance was determined by two-tailed Wilcoxon's matched-pairs signed-rank test with *P*-values $\leqslant 0.05$ considered to be significant.

Surface and intracellular phosphoprotein flow cytometry

To crosslink membrane-bound IL-15 to either the IL-15Ra or the cell membrane, freshly harvested DCs were immediately fixed in 2% paraformaldhyde final concentration for 10 min at 37 °C before proceeding with the usual surface staining protocol. Staining for surface markers was as described above. Intracellular phosphorylated proteins were stained and analyzed as described previously,[36] with the following modifications. imDCs or mDCs were rested for 2 h without cytokines before fixation with 2% paraformaldehyde for 10 min at 37 °C, and permeabilized with cold 90% methanol for 1 h on ice or overnight at − 20 °C, washed and stained with anti-phosphoprotein Abs for 1 h at room temperature. Anti-CD11c Ab was also added along with the phosphoprotein Abs while staining DCs. Data were collected on the BD LSRII flow cytometer and analyzed with FlowJo. MFI and percentage variations (Δ) of phosphoprotein-positive cells were determined by subtracting the nonspecific autofluorescence value from the sample value. Statistical significance for DC surface markers and DC basal level phosphoprotein was determined via two-tailed Wilcoxon's matched-pairs signed-rank test. When smaller number of donors was analyzed, statistical significance for the direct effect of IL-4 or IL-15 during DC maturation was calculated by two-tailed *t*-test. The calculated *P*-values $\leqslant 0.05$ were considered significant for both tests.

Semiquantitative RT-PCR and qRT-PCR

RNA was isolated with Tri-Reagent (Invitrogen) and cDNA was generated from 1 μg isolated total RNA using oligo(dT) primers from Cell-to-cDNA II Kit as directed by the manufacturer (Ambion, Invitrogen). For the semiquantitative RT-PCR, the generated cDNA was serially diluted from 0, 1:10, 1:100 to 1:1000 as the template. Reaction consisted of 1 μl template and 12.5 μl PCR master mix (Promega, Madison, WI, USA), and 2.5 nM of each primer. Reaction conditions were 95 °C for 10 min, then 35 cycles of 95 °C for 30 s, 60 °C for 30 s and 72 °C for 30 s, and followed by a final extension step at 72 °C for 5 min. RT-PCR primers were designed to span two adjacent exons in the desired gene. The sequences for IFN-γ, TNFα, IL-6 and β-actin gene oligonucleotide primers were as follows: IFN-γ forward primer (FP): 5′-TCAGCTCTGCATCGTTTTGG-3′, reverse primer (RP): 5′-GTTCCATTATCCGCTACATCTGAA-3′; TNFα FP: 5′-TCTTCTCGAACCCCGAGTGA-3′, RP: 5′-CCTCTGATGGCACCACCAG 3′; IL-6 FP: 5′-GTAGCCGCCCCACACAGACAGCC-3′, RP: 5′-GCCATCTTT GGAAGGTTCAGG-3′; and β-actin FP: 5′-ACCTTCTACAATGAGCTGCG-3′, RP: 5′-CCTGGATAGCAACGTACATGG-3′.

For quantitative SYBR green real-time PCR (qRT-PCR), the same cDNA and primer sets for IFN-γ, TNFα, and β-actin were used in the qRT-PCR reactions. The IL-6 qRT-PCR FP was 5′-CCACTCACCTCTTCAGAACG-3′ and RP was 5′-TCTGCCAGTGCCTCTTTGC-3′. Amplification of each gene was completed in triplicate reactions, which consisted of 1 μl template, 12.5 μl 2× SYBR green qPCR master mix and determined optimal primer concentration. Optimized primer concentrations used in qRT-PCR reactions were determined to be 500 nM for each primer for IFN-γ and IL-6, 300 nM for each primer for TNFα, and 100 nM of each primer for β-actin. Conditions for the qRT-PCR reaction was conducted as suggested by SABioscience using the MX3000P qPCR system (Stratagene, Agilent Technologies, Santa Clara, CA, USA) at 95 °C for 10 min, followed by 40 cycles of 95 °C for 30 s, 60 °C for 30 s, and followed by a dissociation curve analysis to confirm amplification of a single amplicon. Relative expression levels of the cytokine transcripts were calculated by the $2^{\Delta Ct}$ method and then normalized with the β-actin levels.

Intracellular cytokine staining of DCs and flow cytometry analysis

mDCs were washed, blocked with 10% human and mouse sera for 30 min, stained with anti-CD11c Ab for 30 min, fixed and permeabilized with BD Fix/Perm Buffer, stained with anti-IFN-γ or anti-TNFα for 1 h and then analyzed. Data were collected on the BD LSRII flow cytometer and analyzed with FlowJo. ΔMFI and Δpercentage of $IFN\text{-}\gamma^+$ or $TNF\alpha^+$ from the $CD11c^+$-gated mDC populations were calculated as explained previously. Statistical significance was determined using the two-tailed Wilcoxon's matched-pairs signed-rank test in which calculated *P*-values $\geqslant 0.05$ were considered significant.

CONFLICT OF INTEREST

The authors declare no conflict of interest.

ACKNOWLEDGEMENTS

We thank Neil Benson for help with flow cytometry operation, and David Bloom and Paul Gulig for continued participation in discussion throughout this study. The study was supported by grant from Yongling Foundation, and research fund of UF/Health Cancer Center. Author contributions LJC, SO and SH designed the studies; SO, SH and EP carried out the experiments; SO drafted and LJC revised and finalized the manuscript; LJY participated in the design and discussion of the study; all authors read and approved the final manuscript.

1 Ardavin C, Martinez del Hoyo G, Martin P, Anjuere F, Arias CF, Marin AR *et al.* Origin and differentiation of dendritic cells. *Trends Immunol* 2001; **22**: 691–700.
2 Geissmann F, Manz MG, Jung S, Sieweke MH, Merad M, Ley K. Development of monocytes, macrophages, and dendritic cells. *Science* 2010; **327**: 656–661.
3 Banchereau J, Briere F, Caux C, Davoust J, Lebecque S, Liu YJ *et al.* Immunobiology of dendritic cells. *Annu Rev Immunol* 2000; **18**: 767–811.
4 Jacobs B, Wuttke M, Papewalis C, Seissler J, Schott M. Dendritic cell subtypes and *in vitro* generation of dendritic cells. *Horm Metab Res* 2008; **40**: 99–107.
5 Liu YJ. Dendritic cell subsets and lineages, and their functions in innate and adaptive immunity. *Cell* 2001; **106**: 259–262.
6 Banchereau J, Palucka AK. Dendritic cells as therapeutic vaccines against cancer. *Nat Rev Immunol* 2005; **5**: 296–306.
7 Saikh KU, Khan AS, Kissner T, Ulrich RG. IL-15-induced conversion of monocytes to mature dendritic cells. *Clin Exp Immunol* 2001; **126**: 447–455.
8 Anguille S, Smits EL, Cools N, Goossens H, Berneman ZN, Van Tendeloo VF. Short-term cultured, interleukin-15 differentiated dendritic cells have potent immunostimulatory properties. *J Transl Med* 2009; **7**: 109.
9 Dubsky P, Saito H, Leogier M, Dantin C, Connolly JE, Banchereau J *et al.* IL-15-induced human DC efficiently prime melanoma-specific naive CD8+ T cells to differentiate into CTL. *Eur J Immunol* 2007; **37**: 1678–1690.
10 Hardy MY, Kassianos AJ, Vulink A, Wilkinson R, Jongbloed SL, Hart DN *et al.* NK cells enhance the induction of CTL responses by IL-15 monocyte-derived dendritic cells. *Immunol Cell Biol* 2009; **87**: 606–614.
11 Pulendran B, Dillon S, Joseph C, Curiel T, Banchereau J, Mohamadzadeh M. Dendritic cells generated in the presence of GM-CSF plus IL-15 prime potent CD8+ Tc1 responses *in vivo*. *Eur J Immunol* 2004; **34**: 66–73.
12 Mohamadzadeh M, Berard F, Essert G, Chalouni C, Pulendran B, Davoust J *et al.* Interleukin 15 skews monocyte differentiation into dendritic cells with features of Langerhans cells. *J Exp Med* 2001; **194**: 1013–1020.
13 Budagian V, Bulanova E, Paus R, Bulfone-Paus S. IL-15/IL-15 receptor biology: a guided tour through an expanding universe. *Cytokine Growth Factor Rev* 2006; **17**: 259–280.
14 Tagaya Y, Bamford RN, DeFilippis AP, Waldmann TA. IL-15: a pleiotropic cytokine with diverse receptor/signaling pathways whose expression is controlled at multiple levels. *Immunity* 1996; **4**: 329–336.

15 Han S, Wang Y, Wang B, Patel E, Okada S, Yang L-J *et al. Ex vivo* development, expansion and *in vivo* analysis of a novel lineage of dendritic cells from hematopoietic stem cells. *J Immune Based Ther Vaccines* 2010; **8**: 8.
16 Curtsinger JM, Schmidt CS, Mondino A, Lins DC, Kedl RM, Jenkins MK *et al.* Inflammatory cytokines provide a third signal for activation of naive CD4+ and CD8+ T cells. *J Immunol* 1999; **162**: 3256–3262.
17 Burkett PR, Koka R, Chien M, Chai S, Boone DL, Ma A. Coordinate expression and trans presentation of interleukin (IL)-15Ralpha and IL-15 supports natural killer cell and memory CD8+ T cell homeostasis. *J Exp Med* 2004; **200**: 825–834.
18 Cooper MA, Fehniger TA, Fuchs A, Colonna M, Caligiuri MA. NK cell and DC interactions. *Trends Immunol* 2004; **25**: 47–52.
19 Anguille S, Lion E, Van den Bergh J, Van Acker HH, Willemen Y, Smits EL *et al.* Interleukin-15 dendritic cells as vaccine candidates for cancer immunotherapy. *Hum Vaccin Immunother* 2013; **9**: 1956–1961.
20 Han S, Huang Y, Liang Y, Ho Y, Wang Y, Chang L-J. Phenotype and functional evaluation of *ex vivo* generated antigen-specific immune effector cells with potential for therapeutic applications. *J Hematol Oncol* 2009; **2**: 34.
21 Nelms K, Keegan AD, Zamorano J, Ryan JJ, Paul WE. The IL-4 receptor: signaling mechanisms and biologic functions. *Annu Rev Immunol* 1999; **17**: 701–738.
22 Hunt AE, Williams LM, Lali FV, Foxwell BM. IL-4 regulation of p38 MAPK signalling is dependent on cell type. *Cytokine* 2002; **18**: 295–303.
23 Giron-Michel J, Caignard A, Fogli M, Brouty-Boye D, Briard D, van Dijk M *et al.* Differential STAT3, STAT5, and NF-kappaB activation in human hematopoietic progenitors by endogenous interleukin-15: implications in the expression of functional molecules. *Blood* 2003; **102**: 109–117.
24 Budagian V, Bulanova E, Orinska Z, Pohl T, Borden EC, Silverman R *et al.* Reverse signaling through membrane-bound interleukin-15. *J Biol Chem* 2004; **279**: 42192–42201.
25 Bell BD, Kitajima M, Larson RP, Stoklasek TA, Dang K, Sakamoto K *et al.* The transcription factor STAT5 is critical in dendritic cells for the development of TH2 but not TH1 responses. *Nat Immunol* 2013; **14**: 364–371.
26 Hercus TR, Thomas D, Guthridge MA, Ekert PG, King-Scott J, Parker MW *et al.* The granulocyte–macrophage colony-stimulating factor receptor: linking its structure to cell signaling and its role in disease. *Blood* 2009; **114**: 1289–1298.
27 Giron-Michel J, Giuliani M, Fogli M, Brouty-Boye D, Ferrini S, Baychelier F *et al.* Membrane-bound and soluble IL-15/IL-15Ralpha complexes display differential signaling and functions on human hematopoietic progenitors. *Blood* 2005; **106**: 2302–2310.
28 Park SJ, Nakagawa T, Kitamura H, Atsumi T, Kamon H, Sawa S *et al.* IL-6 regulates *in vivo* dendritic cell differentiation through STAT3 activation. *J Immunol* 2004; **173**: 3844–3854.
29 Melillo JA, Song L, Bhagat G, Blazquez AB, Plumlee CR, Lee C *et al.* Dendritic cell (DC)-specific targeting reveals Stat3 as a negative regulator of DC function. *J Immunol* 2010; **184**: 2638–2645.
30 Nakahara T, Moroi Y, Uchi H, Furue M. Differential role of MAPK signaling in human dendritic cell maturation and Th1/Th2 engagement. *J Dermatol Sci* 2006; **42**: 1–11.
31 Braun DA, Fribourg M, Sealfon SC. Cytokine response is determined by duration of receptor and signal transducers and activators of transcription 3 (STAT3) activation. *J Biol Chem* 2013; **288**: 2986–2993.
32 Laouar Y, Welte T, Fu XY, Flavell RA. STAT3 is required for Flt3L-dependent dendritic cell differentiation. *Immunity* 2003; **19**: 903–912.
33 Ku JL, Kang SB, Shin YK, Kang HC, Hong SH, Kim IJ *et al.* Promoter hypermethylation downregulates RUNX3 gene expression in colorectal cancer cell lines. *Oncogene* 2004; **23**: 6736–6742.
34 Han S, Wang B, Cotter MJ, Yang LJ, Zucali J, Moreb JS *et al.* Overcoming immune tolerance against multiple myeloma with lentiviral calnexin-engineered dendritic cells. *Mol Ther* 2008; **16**: 269–279.
35 Chen X, He J, Chang L-J. Alteration of T cell immunity by lentiviral transduction of human monocyte-derived dendritic cells. *Retrovirology* 2004; **1**: 37.
36 Patel E, Chang L-J. Synergistic effects of interleukin-7 and pre-T cell receptor signaling in human T cell development. *J Biol Chem* 2012; **287**: 33826–33835.

The Supplementary Information that accompanies this paper is available on the Immunology and Cell Biology website (http://www.nature.com/icb)